Remote Preparation of Arbitrary Time-Encoded Single-Photon Ebits

Alessandro Zavatta,[1] Milena D'Angelo,[2] Valentina Parigi,[3] and Marco Bellini[1,2,*]

[1]*Istituto Nazionale di Ottica Applicata, CNR, Largo Enrico Fermi, 6, I-50125 Florence, Italy*
[2]*LENS, Via Nello Carrara 1, 50019 Sesto Fiorentino, Florence, Italy*
[3]*Department of Physics, University of Florence, I-50019 Sesto Fiorentino, Florence, Italy*
(Received 8 September 2005; published 18 January 2006)

We propose and experimentally verify a novel method for the remote preparation of entangled bits (ebits) made of a single photon coherently delocalized in two well-separated temporal modes. The proposed scheme represents a remotely tunable source for tailoring arbitrary ebits, whether maximally or nonmaximally entangled, which is highly desirable for applications in quantum information technology. The remotely prepared ebit is studied by performing homodyne tomography with an ultrafast balanced homodyne detection scheme recently developed in our laboratory.

Entanglement, nonlocal correlations, indistinguishable alternatives are historically among the most intriguing and appealing topics of quantum mechanics. Besides their relevance in fundamental physics [1], these phenomena have attracted much attention due to their usefulness in quantum information technology [2]. Extravagant but promising protocols such as quantum teleportation, quantum cryptography, and quantum computation have been proposed and experimentally verified (see, e.g., [2], and references therein). All these schemes were originally based on two-photon entanglement. Recently, increasing attention has been given to a new quantum information perspective: the carriers of quantum information are no longer the photons, but rather the field modes "carrying" them. Based on this idea, two different approaches have been followed. The first one exploits the entanglement in momentum generated when a single photon impinges on a beam splitter and is characterized by the state $\alpha|1\rangle_a|0\rangle_b + \beta|0\rangle_a|1\rangle_b$, where a and b denote two distinct spatial modes and α and β are complex amplitudes such that $|\alpha|^2 + |\beta|^2 = 1$ (see, e.g., [3,4], and references therein). The second and more recent road has been traced by Gisin's group [5] on the line of Franson's approach [6], and leads to two-photon systems entangled in ultrashort copropagating temporal modes (or "time bins") [7].

In this Letter, we propose the first remotely tunable source of arbitrary single-photon entangled states (ebits) in the time domain and experimentally demonstrate its working principle. We start from the spontaneous parametric down conversion (SPDC) signal-idler pairs [8] generated by a train of phase-locked pump pulses [5,9] and generate indistinguishability between pairs of consecutive nonoverlapping temporal modes propagating in the idler channel; this enables us to remotely delocalize the twin signal photon between two identical and well-separated time bins, thus generating the single-photon temporal ebit: $\alpha|1^{(n)}\rangle|0^{(n+1)}\rangle + \beta|0^{(n)}\rangle|1^{(n+1)}\rangle$, where n denotes the temporal mode associated with the nth pump pulse. Both maximally and nonmaximally entangled single-photon

states, with any relative phase, can be produced by performing simple and reversible operations in the remote idler channel. The proposed scheme may find immediate application in quantum information technology; single-photon ebits have been proven to enable linear optics quantum teleportation [3,10] and play a central role in linear optics quantum computation [4,11]. Furthermore, time-bin entanglement has been proven suitable for long distance applications [10,12], where the insensitivity to both depolarization and polarization fluctuations becomes a strong requirement. In addition, since the carriers of entanglement are naturally separated (i.e., no further optical element is required) and undergo the same losses, entanglement in time is less sensitive to losses and easier to purify [13].

The experimental setup is pictured in Fig. 1. The 1.5 ps pulses at 786 nm from a mode-locked Ti:Sapphire laser at a repetition rate of 82 MHz are frequency doubled in a LBO crystal. The resulting pulse train impinges on a nonlinear BBO crystal cut for degenerate ($\Omega_s = \Omega_i = \Omega_p/2$) noncollinear type-I SPDC; signal-idler photon pairs centered at 786 nm are thus generated in two distinct spatial modes. A single-mode fiber and a pair of etalon interference filters (F) are employed for spatial and spectral filtering of the
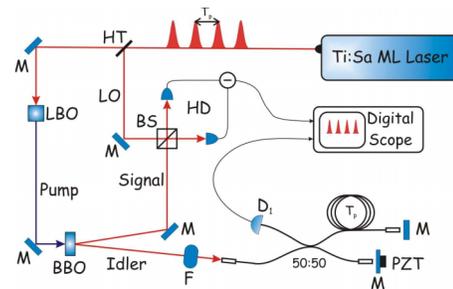

FIG. 1 (color online). Schematic representation of the experimental setup. 50–50 is a 3 dB fiber coupler, HT a high-transmission beam splitter, and M are mirrors. See text for further details.

idler beam before its entrance in a fiber-coupled piezoco-trolled (PZT) Michelson interferometer; a single-photon detector (D_1) is inserted at the exit port of the interferometer. The signal beam propagates in free space before being mixed at a 50–50 beam splitter (BS) with a local oscillator (LO) for high-frequency time-domain balanced homodyne detection (HD) [14,15]. Spatial and spectral filtering of the idler mode guarantees the conditional projection of the signal photons into a single-photon pure state [16–18]. On the other hand, the Michelson interferometer generates indistinguishability between two consecutive temporal modes propagating in the idler channel: an idler photon detected by D_1 may have been generated by either the Nth or the $(N + 1)$th pump pulse, provided that the time delay (T) between the short and long arms of the interferometer is chosen to be approximately equal to the time separation between two consecutive pump pulses ($T_p = 12.3$ ns). Notice that the bandpass of the spectral filter in the idler arm ($\sigma_i = 50$ GHz) is wide enough so that no first order interference occurs ($\sigma_i \gg \pi/T_p$).

Based on a standard quantum mechanical calculation, we find that the combination of indistinguishability and tight filtering in the idler channel allows the conditional remote preparation, in the signal channel, of the temporally delocalized single-photon ebit:

$$|\Psi_s^{\phi_i}\rangle = \frac{1}{\sqrt{2}}(|1^{(n)}, 0^{(n+1)}\rangle + e^{-i\phi_i}|0^{(n)}, 1^{(n+1)}\rangle), \quad (1)$$

with $\phi_i = \Omega_p(T_p - T/2)$. Interestingly, the relative phase ϕ_i characterizing the remotely prepared ebit is defined not only by the phase difference introduced by the Michelson interferometer ($\varphi_{\text{int}} = \Omega_i T$), but also by the relative phase between consecutive pump pulses ($\varphi_{\text{pump}} = \Omega_p T_p$). The result of Eq. (1) represents the temporal counterpart of the spatially delocalized single photon produced at the output ports of a beam splitter; this case has been studied experimentally by Babichev *et al.* [19]. However, different from Ref. [19], the entangled state of Eq. (1) has been prepared remotely, without performing any manipulation on the signal photons. It is the interferometer in the idler arm which generates indistinguishability between two consecutive nonoverlapping temporal modes; this indistinguishability, together with the coherence of both pump beam and SPDC process, gives rise, in the signal channel, to the coherent superposition of two previously independent and still temporally separated time bins. An important advantage of such a remote state preparation scheme is the possibility of generating both maximally and nonmaximally single-photon entangled states, with any relative phase ϕ_i, by performing simple and reversible operations in the idler arm (or on the train of pump pulses). For instance, two of the four Bell states, namely, $|\Psi_s^\pm\rangle = \frac{1}{\sqrt{2}} \times (|1^{(n)}, 0^{(n+1)}\rangle \pm |0^{(n)}, 1^{(n+1)}\rangle)$, can be easily generated by manipulating the interferometer. Furthermore, the probability amplitudes characterizing the delocalized single pho-

ton may be continuously varied by simply introducing controllable losses in one arm of the interferometer; this has the only effect of lowering the production rate but does not introduce any impurity in the state generated in the signal channel.

The expected two-mode Wigner function [20] for the delocalized single photon of Eq. (1) is given by

$$W^{\phi_i}(x_1, y_1; x_2, y_2) = \frac{1}{2}[8W_{10}^{\phi_i}(x_1, y_1; x_2, y_2)$$
$$+ W_1(x_1, y_1)W_0(x_2, y_2)$$
$$+ W_0(x_1, y_1)W_1(x_2, y_2)], \quad (2)$$

where $W_1(x, y) = \frac{2}{\pi}e^{-2x^2}e^{-2y^2}(4x^2 + 4y^2 - 1)$ and $W_0(x, y) = \frac{2}{\pi}e^{-2x^2}e^{-2y^2}$ are the single-mode Wigner functions associated with a single-photon Fock state and with the vacuum, respectively; on the other hand, $W_{10}^{\phi_i}(x_1, y_1; x_2, y_2)$ is a nonfactorable 4D function which couples the quadratures of two consecutive nonoverlapping signal temporal modes:

$$W_{10}^{\phi_i}(x_1, y_1; x_2, y_2) = W_0(x_1, y_1)W_0(x_2, y_2)(x_1 x_2^{\phi_i} + y_1 y_2^{\phi_i}), \quad (3)$$

where $x_2^{\phi_i} = x_2\cos\phi_i - y_2\sin\phi_i$ and $y_2^{\phi_i} = x_2\sin\phi_i + y_2\cos\phi_i$. Then, the Wigner function associated with the delocalized signal photon contains information about the characteristic phase ϕ_i introduced through the idler arm. Also notice that, by introducing the phase-dependent correlation quadratures $x_\pm^{\phi_i} = (x_1 \pm x_2^{\phi_i})/\sqrt{2}$ and $y_\pm^{\phi_i} = (y_1 \pm y_2^{\phi_i})/\sqrt{2}$, the Wigner function of Eq. (2) factors:

$$W(x_+^{\phi_i}, y_+^{\phi_i}; x_-^{\phi_i}, y_-^{\phi_i}) = W_1(x_+^{\phi_i}, y_+^{\phi_i})W_0(x_-^{\phi_i}, y_-^{\phi_i}). \quad (4)$$

This result explicitly indicates that the delocalized single photon cannot be described in terms of the quadratures associated with neither one of the two distant temporal modes (1 and 2), separately; however, the single photon is well defined in the phase space $(x_+^{\phi_i}, y_+^{\phi_i})$, while the vacuum is defined in the phase space $(x_-^{\phi_i}, y_-^{\phi_i})$. Thus, the 4D Wigner function reproduces the correlations remotely generated between pairs of well-separated temporal modes in the signal arm.

We have experimentally verified the correctness of the above predictions by performing balanced homodyne tomography and reconstructing both the density matrix and the Wigner function of the ebit remotely prepared in the signal channel. The density matrix has been reconstructed directly from the homodyne data by employing the method developed by D'Ariano *et al.* [21]; its elements have then been used to reconstruct the Wigner function (for more details, see our previous works [15,22]).

In order to reconstruct the two-mode 4D Wigner function of Eq. (2), one would normally need to measure the joint marginal distribution of the quadratures $X_1(\theta_1) = x_1\cos\theta_1 - y_1\sin\theta_1$ and $X_2(\theta_2) = x_2\cos\theta_2 - y_2\sin\theta_2$,

while varying the phases θ_1 and θ_2 of two LO pulses spatially and temporally matched (i.e., synchronized) to the modes 1 and 2, respectively. However, the particular state investigated here is invariant with respect to the global phase, and only the relative phase $\Delta\theta = \theta_1 - \theta_2$ needs to be controlled in the experiment [19,20]. Moreover, the joint marginal distribution is invariant under interchange of ϕ_i and $\Delta\theta$. We exploited this property in order to overcome the difficulty connected to the generation of a pair of phase-controllable LO pulses out of the train coming from the laser. Rather than varying the relative LO phase, one may keep $\Delta\theta$ fixed (by just using any two consecutive pulses directly from the mode-locked train) and vary the phase ϕ_i by means of the interferometer. Although what we actually do in this case is to measure fixed quadratures on the two modes for a varying quantum state $|\Psi_s^{\phi_i}\rangle$, it is immediate to show that this is equivalent to performing a conventional LO phase scan of the fixed quantum state $|\Psi_s^{\phi_i=\text{const}}\rangle$. We shall name this technique "remote balanced homodyne tomography."

For each value of the interferometer phase φ_{int} and upon detection of an idler photon, stable and fast quadrature measurements have been realized on the corresponding pair of consecutive signal time bins (plus one containing just the vacuum and used for calibration), while keeping both the local oscillator and the homodyne detection apparatus unchanged. A total of 10^6 quadrature measurements, equally distributed over the range $[0, \pi]$ of φ_{int}, has been performed on each of the three time bins. The experimental results are reported in Fig. 2, where we plot the measured values of the quadratures X_1 and X_2 obtained for three different values of the remote phase ϕ_i, while leaving $\Delta\theta$ fixed. According to the above reasoning, these results also represent the marginal distributions $p(X_1, X_2, \Delta\theta)$ associated with the ebit of Eq. (1) for $\phi_i =$

0, and obtained for three different values of the relative phase $\Delta\theta$. Notice that, while the joint distribution $p(X_1, X_2, \Delta\theta)$ is strongly phase dependent, the marginal distributions $p(X_1)$ and $p(X_2)$ associated with each temporal mode, separately, are phase independent. This is consistent with the fact that each mode, separately, is an incoherent statistical mixture of vacuum and single-photon Fock state; however, the pair of modes 1 and 2, as a whole, is in the coherent superposition described by Eq. (1), with $\phi_i = 0$. Figure 2 also shows that a single-photon Fock state is defined in the phase space $(x_+^{\phi_i=0}, y_+^{\phi_i=0})$, while the vacuum is defined in the phase space $(x_-^{\phi_i=0}, y_-^{\phi_i=0})$, as expected from Eq. (4).

Figure 3(a) reports the reconstructed density matrix: $\hat{\rho} = (1 - \eta)|0\rangle\langle 0| + \eta|\Psi_s^{\phi_i=0}\rangle\langle\Psi_s^{\phi_i=0}|$, where the overall efficiency $\eta = 60.5\%$ accounts for both preparation and detection efficiencies; notice that almost no multiphoton contribution exists. From this figure it is also apparent that the vacuum contamination, hence the losses, does not degrade the coherence of the remotely delocalized single photon; in fact, both the nondiagonal and the diagonal ($|01\rangle\langle 01|$ and $|10\rangle\langle 10|$) elements of the reconstructed density matrix are reduced by the same amount. This may be understood as a consequence of the common losses undergone by the pair of entangled time bins. Figures 3(b) and 3(c) reproduce, respectively, the (x_1, y_1) and (x_1, x_2) sections of the reconstructed 4D Wigner function $W^{\phi_i=0}(x_1, y_1, x_2, y_2)$. The cross section (x_1, y_1) resembles the standard Wigner function of a single-photon Fock state, but is characterized by a well-defined phase; the existence of this phase is the result of the coherent delocalization of the single photon between two separate temporal modes. The (x_1, x_2) section of the reconstructed Wigner function explicitly shows the correlation between the quadratures x_1 and x_2; the nonfactorable nature of the delocalized single photon is here apparent.
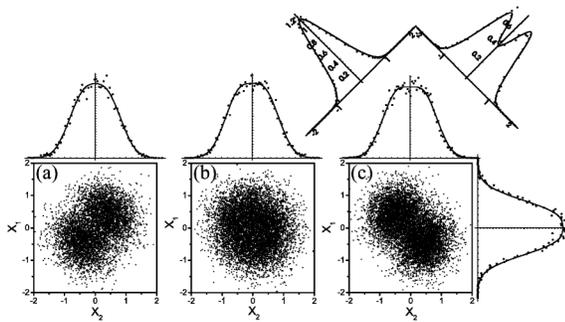

FIG. 2. Joint marginal distributions of the measured two-mode field quadratures for: (a) $\phi_i = -\Delta\theta$, (b) $\phi_i = \pi/2 - \Delta\theta$, (c) $\phi_i = \pi - \Delta\theta$, while leaving $\Delta\theta$ fixed. These are also the joint marginal distributions $p(X_1, X_2, \Delta\theta)$ associated with the ebit of Eq. (1) for $\phi_i = 0$, and corresponding, respectively, to $\Delta\theta = 0, \pi/2, \pi$. The histograms are the single-mode marginal distributions $p(X_1)$ and $p(X_2)$ together with the corresponding best fits. The marginals for the $x_\pm$ quadratures are plotted on the diagonal axes above (c).
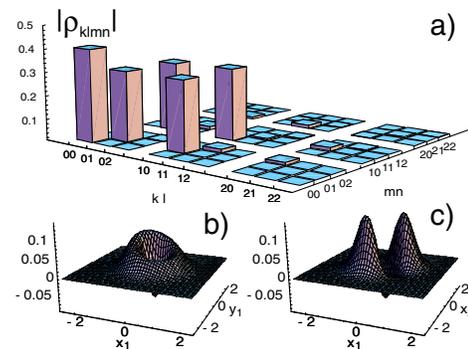

FIG. 3 (color online). (a) Reconstructed density matrix elements $\rho_{klmn} = \langle k_1 l_2|\hat{\rho}|m_1 n_2\rangle$ corresponding to the state of Eq. (1) with $\phi_i = 0$. Cross sections of the reconstructed 4D Wigner function: (b) $W^{\phi_i=0}(x_1, y_1; -0.1, -0.1)$, and (c) $W^{\phi_i=0}(x_1, 0; x_2, 0)$.
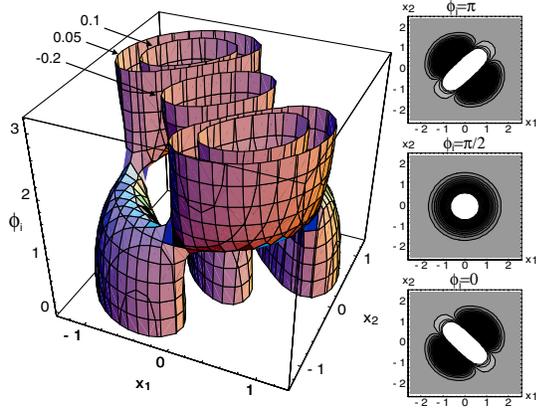
FIG. 4 (color online). Three-dimensional contour plot of the Wigner function section $W^{\phi_i}(x_1, 0, x_2, 0)$ associated with the single-photon ebit of Eq. (1) versus its characteristic remotely tunable phase ϕ_i. The surfaces shown correspond to three values of the Wigner function, namely: $W^{\phi_i} = -0.2, 0.05, 0.1$. Insets: contour plots for three specific values of the phase ϕ_i.

In summary, the experimental reconstruction of the Wigner function of the conditionally prepared single-photon ebit has enabled us to verify its entangled nature and study its purity. Besides the nonclassical behavior typical of single-photon Fock states (negative values around the origin), the reconstructed 4D Wigner function has been found to be characterized by an intriguing phase information and by correlation between well-separated temporal modes, as expected from Eq. (2). It may seem counterintuitive that a single photon simultaneously affects two nonoverlapping temporal modes or, equivalently, carries a well-defined phase. However, the effect is a direct consequence of the coherent superposition remotely induced between otherwise independent signal time bins; it can then be understood in terms of quantum entanglement between two copropagating but distinct temporal modes carrying a single photon.

From the applicative viewpoint, one of the most interesting aspects of the proposed scheme is the dependence of the relative phase characterizing the delocalized (signal) single photon on both the relative phase between pump pulses and the phase delay introduced by the remote Michelson interferometer. Based on this effect, for any fixed value of the remotely controlled phase ϕ_i, one may generate, in the signal arm, a specific single-photon ebit. This point is pictorially demonstrated by Fig. 4, where we draw the contour plots of the (x_1, x_2) section of the 4D Wigner function for all possible values of the remotely tunable phase ϕ_i characterizing the ebit of Eq. (1). The Wigner function $W^{\phi_i}(x_1, 0; x_2, 0)$ associated with each conditionally prepared ebit $|\Psi_s^{\phi_i}\rangle$ reveals a specific correlation between the field quadratures of two distinct signal temporal modes; as the preparation phase ϕ_i is changed from 0 to π, we observe the transition from correlated to anticorrelated quadratures through a "saddle" point at

$\phi_i = \pi/2$, where the anticorrelation is transferred into the quadrature space (x_1, y_2) (not shown in figure). In other words, the proposed scheme can be regarded as a remotely tunable source of arbitrary single-photon ebits; such a source is highly desirable for applications in quantum information technology.

*Electronic address: bellini@inoa.it

[1] A. Einstein, B. Podolsky, and N. Rosen, Phys. Rev. **47**, 777 (1935); J. S. Bell, Physics (Long Island City, N.Y.) **1**, 195 (1964).

[2] C. H. Bennett and B. D. DiVincenzo, Nature (London) **404**, 247 (2000).

[3] S. Giacomini *et al.*, Phys. Rev. A **66**, 030302 (2002).

[4] E. Knill, R. Laflamme, and G. J. Milburn, Nature (London) **409**, 46 (2001).

[5] J. Brendel *et al.*, Phys. Rev. Lett. **82**, 2594 (1999); H. de Riedmatten *et al.*, Phys. Rev. A **69**, 050304 (2004).

[6] J. D. Franson, Phys. Rev. Lett. **62**, 2205 (1989).

[7] C. Simon and J.-P. Poizat, Phys. Rev. Lett. **94**, 030502 (2005).

[8] D. N. Klyshko, *Photon and Nonlinear Optics* (Gordon and Breach Science, New York, 1988).

[9] T. E. Keller and M. H. Rubin, Phys. Rev. A **56**, 1534 (1997); Y.-H. Kim *et al.*, Phys. Rev. A **62**, 043820 (2000).

[10] H. de Riedmatten *et al.*, Phys. Rev. Lett. **92**, 047904 (2004).

[11] T. B. Pittman, B. C. Jacobs, and J. D. Franson, Phys. Rev. A **71**, 032307 (2005).

[12] W. Tittel, J. Brendel, H. Zbinden, and N. Gisin, Phys. Rev. Lett. **84**, 4737 (2000).

[13] I. L. Chuang and Y. Yamamoto, Phys. Rev. Lett. **76**, 4281 (1996).

[14] A. Zavatta *et al.*, J. Opt. Soc. Am. B **19**, 1189 (2002).

[15] A. Zavatta, S. Viciani, and M. Bellini, Phys. Rev. A **70**, 053821 (2004).

[16] T. Aichele, A. I. Lvovsky, and S. Schiller, Eur. Phys. J. D **18**, 237 (2002).

[17] M. Bellini *et al.*, Phys. Rev. Lett. **90**, 043602 (2003).

[18] S. Viciani, A. Zavatta, and M. Bellini, Phys. Rev. A **69**, 053801 (2004).

[19] S. A. Babichev, J. Appel, and A. I. Lvovsky, Phys. Rev. Lett. **92**, 193601 (2004).

[20] U. Leonhardt, *Measuring the Quantum State of Light* (Cambridge University Press, Cambridge, 1997).

[21] G. M. D'Ariano, C. Macchiavello, and M. G. A. Paris, Phys. Rev. A **50**, 4298 (1994).

[22] A. Zavatta, S. Viciani, and M. Bellini, Science **306**, 660 (2004); Phys. Rev. A **72**, 023820 (2005).